Electronic Supplementary Information for Dalton Transactions

Electronic Supplementary Information

belonging to the paper

The structural effects of the Cys-S-S-Cys bridge exchange by the His-Cu(II)-His motif studied on natural peptides – a promising tool for natural compounds-based design

Justyna Brasuń,[a*] Marek Cebrat,[b] Łukasz Jaremko,[c,d] Mariusz Jaremko,[c] Gregor Ilc,[e] Olimpia Gładysz[a] and Igor Zhukov [c,e]

[a] *Department of Inorganic Chemistry, Wrocław Medical University, Szewska 38, 50-139 Wrocław, Poland, tel.+48-071-784-03-30, fax +48-071-784-03-36,*

[b] *Faculty of Chemistry, University of Wrocław, F. Joliot- Curie 14, 50-383 Wrocław, Poland*

[c] *Institute of Biochemistry and Biophysics, Polish Academy of Sciences, Pawińskiego 5a, 02-106, Warsaw, Poland*

[d] *Institute of Genetics and Biotechnology, Warsaw University, Pawińskiego 5A, 02-106 Warsaw, Poland*

[e] *Slovenian NMR Center, National Institute of Chemistry, Hajdrihova 19, SI-1000 Ljubljana, Slovenia*

E-mail: jbrasun@chnorg.am.wroc.pl

Synthetic Procedures and Full Experimental Details

Peptide Synthesis

Peptides were obtained by the manual solid phase synthesis method on the Rink amide resin (0.61 mmol/g, Iris Biotech GmBH) using standard Fmoc procedures. After completion of the peptide sequence, the crude products were cleaved from the resin by "Reagent K" (TFA : phenol : H_2O : thioanisole : ethanedithiol; 82.5: 5 : 5 : 5 : 2.5) for 2 hours at r.t., precipitated into cold diethyl ether, filtered and washed with ether, dissolved in water and liophilized. Peptides were purified by semipreparative C-18 reversed phase HPLC (Varian ProStar system). The chemical identity of the products was confirmed by ESI-MS (Bruker micrOTOF-Q spectrometer).

Potentiometric Studies

Stability constants were calculated from titration curves. Titrations were carried out at 25°C using sample volumes of 1.5 ml. The ligand concentration was 1×10^{-3} M and the metal-to-ligand ratio was 1:2.

The pH-metric titrations were performed in 0.1 M KNO_3 on a MOLSPIN pH-meter system using a Mettler Toledo InLab 422 semi-micro combined electrode calibrated in hydrogen ion concentration using HNO_3. Stability constants $\beta_{pqr} = [M_pH_qL_r]/[M]^p[H]^q[L]^r$ and stoichiometry of complexes were calculated with the SUPERQUAD program.[1] Standard deviations quoted were also computed by SUPERQUAD and referred to random errors only.

Absorption, CD and EPR spectroscopic measurements

Absorption spectra were recorded on a Perkin–Elmer Lambda Bio 20 spectrophotometer, circular dichroism (CD) spectra on a JASCO J715 spectropolarimeter in the 200-850 nm range, and electron paramagnetic resonance (EPR) spectra on a Bruker ESP 300E

spectrometer at X-band frequency (9.4 GHz) at 120 K. Concentration of the ligand was 1×10^{-3} M and the metal-to-ligand ratio was 1:2.

NMR studies

Sample preparation and sequential assignment. NMR samples of both peptides were prepared in H_2O/D_2O (9:1, v:v) solution. The concentrations of the peptides were 3.2 mM and 2.8 mM for [$His^{1,6}$]OXT and [$His^{1,6}$]AVP, respectively. The pH was adjusted to 6.0 ± 0.2 (uncorrected value) by adding small amount of 0.1 M NaOH stock solution. The desired concentrations of Cu(II) ions were obtained by adding adequate volumes of stock $CuSO_4$ solution, the pH was checked and adjustedafter every addition, if needed.

All NMR experiments were performed at 28°C on 18.8 T Varian VNMRS NMR spectrometer (^{1}H frequence 799.806 MHz) equipped with four channels, z-gradients PFG unit, and $^1H/^{13}C/^{15}N$ probehead. The recorded 1D ^{1}H NMR spectra were processed and analyzed by VnmrJ software (Varian Inc., Palo Alto, USA). The acquired two-dimensional homo- and heteronuclear NMR spectra were processed by NMRPipe[2] and analyzed with Sparky[3] programs. Assignments of ^{1}H, ^{13}C, and ^{15}N resonances for both, [$His^{1,6}$]OXT and [$His^{1,6}$]AVP peptides were done by application of standard procedure[4] based on inspection of two-dimensional homonuclear TOCSY (with mixing times 10 ms and 90 ms) and ROESY (with mixing time 200 and 500 ms) experiments supplemented by 2D heteronuclear ^1H-^{13}C HSQC and ^1H-^{15}N HSQC spectra recorded on natural abundances of ^{13}C and ^{15}N nuclei (see *Supplementary Data BMRB format files*).

Measurements of spin lattice relaxation rates (R_1). Spin-lattice relaxation rates (R_1) for protons of both peptides with and without 0.02 equivalents of Cu(II) ions were measured with inversion recovery (IR) pulse sequence for isolated peaks in 1D ^{1}H NMR spectrum. The R_1 values were determined by a two-parameter fit of peak intensities to the following equation with the error not bigger than 3%:

$$I(\tau) = I(0)[1 - 2\exp(-\tau R_1)]$$

where $I(0)$ is initial intensity, and τ is interval between π and $\pi/2$ pulses in pulse sequence. The obtained experimental spin-lattice R_1 relaxation times are presented in Table 3.

Determination of metal-proton distances (r). The presence of the paramagnetic ion in the Cu(II)–peptide complex manifests in a selective peak broadening (Figure 1) and changes of spin-lattice relaxation rates.[5] The paramagnetic contribution in the spin-lattice relaxation (R_{1b}) can be described by the following equation:[5]

$$R_{1b} = R_{1obs} - p_f R_{1f} = p_b / \left(R_{1b}^{-1} + \tau_M\right)$$

where $\tau_M = k_{off}^{-1}$ is the residence time of peptide molecules in the metal coordination sphere, p_f and p_b are the fractions of free and bound peptides, R_{1obs} and R_{1f} are the spin-lattice relaxation rates measured after the addition of Cu(II) and in the metal-free solution, respectively, and R_{1b} is the spin-lattice relaxation rate of Cu(II)-bound ligand.

The distance between metal ion and peptide protons (r) can be evaluated based on the Solomon-Bloembergen-Morgan equation[6] which expresses the value of R_{1b} as a function of the metal-proton distance r and and overall correlation time τ_c. In case of Cu(II) cation (S = ½) the Solomon-Bloembergen-Morgan equation could be written as:

$$R_{1b} = \frac{1}{10}\left(\frac{\mu_0}{4\pi}\right)^2 \frac{\hbar^2 \gamma_I^2 \gamma_S^2}{r^6}\left\{\frac{\tau_c}{1+(\omega_I - \omega_S)^2\tau_c^2} + \frac{3\tau_c}{1+\omega_I^2\tau_c^2} + \frac{6\tau_c}{1+(\omega_I + \omega_S)^2\tau_c^2}\right\}$$

where μ_0 is a permeability constant *in vaccuo*, γ_I and γ_S are the proton and electron magnetogyric ratios respectively, ω_I i ω_S are proton and electron Larmor frequencies, r is the distance between proton and Cu(II) cation, and τ_c is a correlation time.

Assuming that Cu(II) cation is coordinated by $N^{\delta 1}$ nitrogens of histidines we could postulate that the distance between Cu(II) and imidazole ring $H^{\varepsilon 1}$ proton is equal to 3.1 Å. The overall correlation time (τ_c), which is connected with the molecule rotation in the solution, can be

estimated from the various hydrodynamic theories. Presented τ_c calculation is based on the Stokes law:[7]

$$\tau_c = \frac{4\pi\eta_w r_H^3}{3k_B T}$$

in which: η_w is solvent viscosity, r_H – the effective hydrodynamic radius, T – temperature, and k_B – Boltzmann's constant. The hydrodynamic radius (r_H) is given by the following equation:[7]

$$r_H = \left(\frac{3VM}{4\pi N}\right)^{1/3} + r_W$$

where r_W is a correction coming from solvation, V is the specific volume of the peptide, which is 0.73 cm^3g^{-1}, M is the molecular weight of the peptide and N is Avagadro's number. Nevertheless, because the estimated distance depends upon the sixth root of the correlation time τ_c, the distances obtained from the Solomon-Bloembergen-Morgan equation will be relatively insensitive to a modest error in the value of τ_c, e.g. the 400% error in τ_c would result in about 1 Å error on distance.

Structure calculations. The structure calculations were performed with a CNS 1.2 software[8] by the standard protocol including simulated annealing, slow cooling procedure followed by the final refinement. The paramagnetic contributions, R_{1b}, were converted into averaged distance constraints (see above) and were used for structure calculations. The list of the distance constraints is presented in Table 1. Finally, 20 out of the 500 initial structures submitted for calculations were selected as representative structures of [$His^{1,6}$]OXT and [$His^{1,6}$]AVP peptides based on the lowest energies criterion. The quality of the resulting structures ensemble was examined by PROCHECK-NMR (v.3.4) program.[9] Figures presenting the structures of the investigated peptides were prepared using MolMol program.[10] The pdb files of [$His^{1,6}$]OXT and [$His^{1,6}$]AVP peptides can be obtained as *Supplementary PDB files*.

Supplementary references.

1 P. Gans, A. Sabatini, A. Vacca, *J. Chem. Soc. Dalton Trans.*, 1985,1195-1199.
2 F. Delaglio, S. Grzesiek, G.W. Vuister, G. Zhu, J. Pfeifer, A. Bax, *Biomol. NMR*. 1995, **6**, 277-293.
3 T.D. Goddard, D.G. Kneller, *2003 SPARKY 3*, University of California, San Francisco.
4 K. Wüthrich, 1986, NMR of proteins and nucleic acids, John Wiley & Sons, New York, USA.
5 P. Stanczak, D. Valensin, P. Juszczyk, Z. Grzonka, C. Migliorini, E. Molteni, G. Valensin, E. Gaggelli, H. Kozłowski, *Biochemistry*, 2005, **44**, 12940-12954.
6 I. Solomon, *Phys. Rev.*, 1955, **99**, 559-565.
7 J. Jacob, B. Baker, R.G. Bryant, D.S. Cafiso, *Biophys. J.*, 1999, **77**, 1086-1092.
8 (a) A.T. Brünger, P.D. Adams, G.M. Clore, P. Gros, R.W. Grosse-Kunstleve, J.S. Jiang, J. Kuszewski, M. Nilges, N.S. Pannu, R.J. Read, L.M. Rice, T. Simonson, G.L. Warren, *Acta Cryst. D*, 1998, **54**, 905-921. (b) A.T. Brünger, *Nature Prot.*, 2007, 2, 2728-2733.
9 R.A. Laskowski, J.A. Rullmann, M.W. MacArthur, R. Kaptein, J.M. Thornton, *J. Biomol. NMR*, 1996, **8**, 477-486.
10 R. Koradi, M. Billeter, K. Wüthrich,; *J. Mol. Graph.*, 1996 **14**, 51-55.

Supplementary figures.

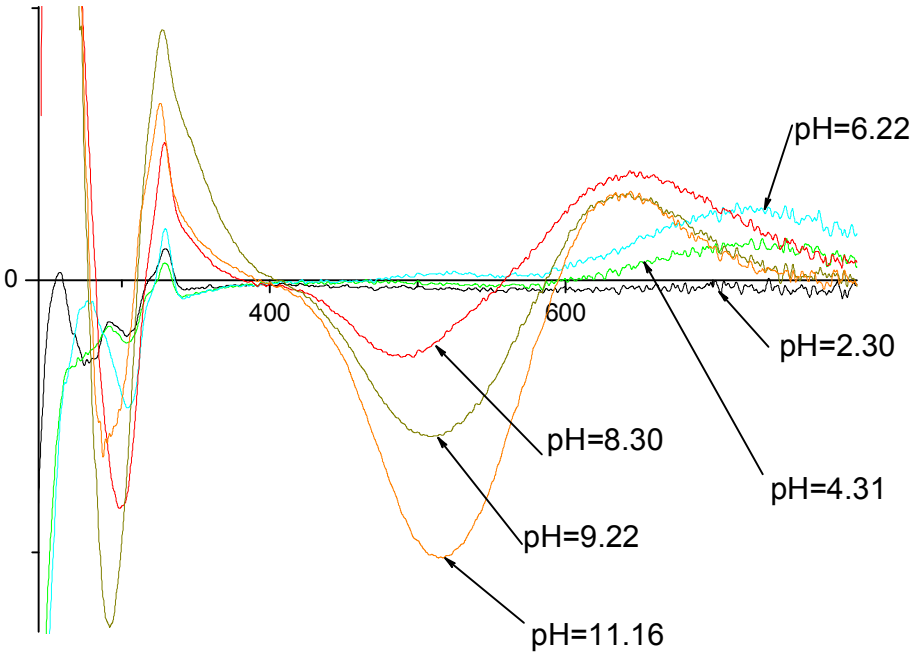

Figure S1. CD spectra of Cu^{2+}/[$His^{1,6}$]OXT complexes. Ligand concentration 1×10^{-3}mol/dm^3, ligand to metal ratio 2:1.

a).

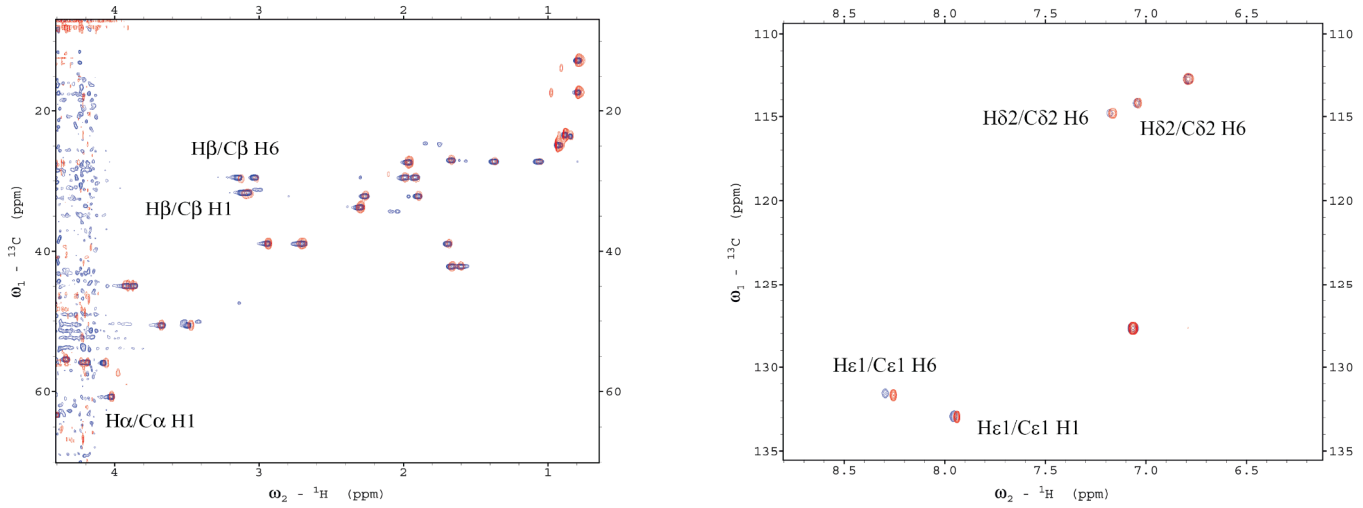

b).

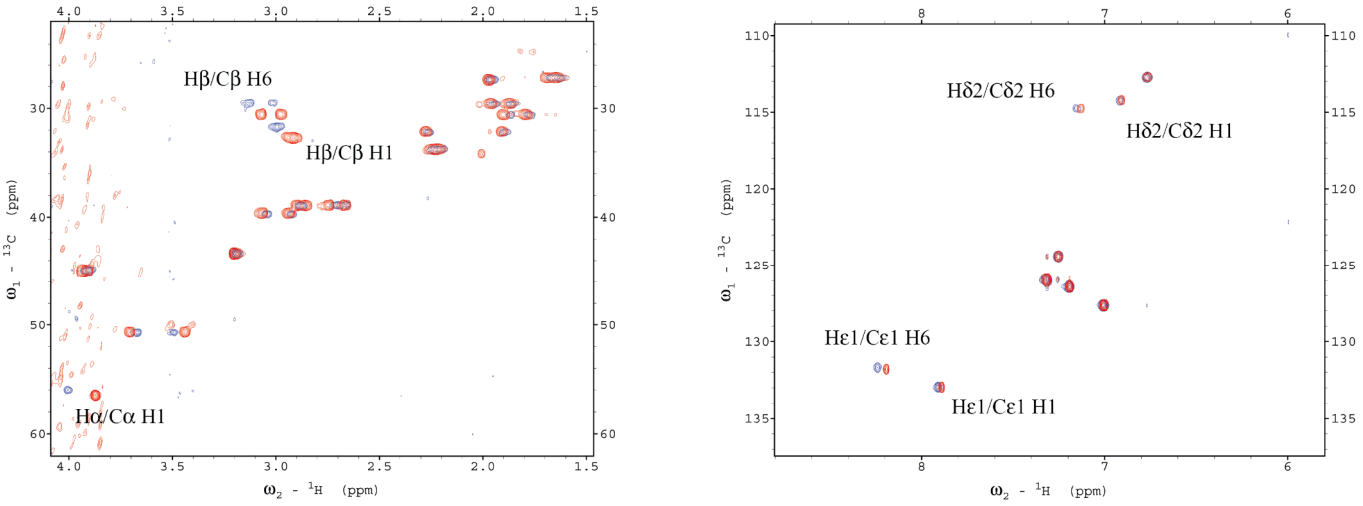

Figure S2. The aliphatic (left) and aromatic (right) ^{1}H-^{13}C HSQC experiments for a) [His^{1,6}]OXT and b) [His^{1,6}]AVP peptides. Red cross-peaks correspond to the free peptide, blue ones are spectra recorded for samples after the addition of 0.02 equivalents of Cu(II) ions. In case of [His^{1,6}]OXT peptide, the addition of Cu(II) does not significantly influence chemical shifts of aliphatic cross-peak resonances, but causes a decrease in the intensities of peaks, which indicates that the chemical exchange process between the ligand and metal is slower than in cause of [His^{1,6}]AVP. The intensities of the same cross peaks for the

[$His^{1,6}$]AVP peptide corresponding to the Hβ/Cβ of histidine residues do not change after addition of the Cu(II) ions, however, the chemical shifts of these peaks undergo noticeable changes. These results are consistent with the ratio of residence times of the peptide molecules in the metal coordination sphere of τ_M[$His^{1,6}$]OXT/τ_M[$His^{1,6}$]AVP ≈ 6, which clearly supports the conclusions taken from 2D experiments analysis. After the further addition of Cu(II) ions the signals of imidazole protons from histidines involved in the coordination of metal disappear in both cases due to the paramagnetic effect.

Supplementary tables.

Table S1. The stability constants for the free ligands: [His^{1,6}]AVP and [His^{1,6}]OXT and for their Cu(II)-complexes.

Species	logβ (free ligand)	
	[His^{1,6}]OXT	[His^{1,6}]AVP
HL	9.52±0.01	11.39
H_2L	16.73±0.01	21.00
H_3L	22.99±0.01	28.29
H_4L	28.13±0.01	34.55
H_5L	-	39.71
log K_{Arg}	-	11.39
log K_{Tyr}	9.52	9.61
log K_{NH2}	7.21	7.29
log K_{Im}	6.26	6.25
log K_{Im}	5.14	5.17
Species	logβ (Cu^{2+} complexes)	
CuH_4L	-	39.60
CuH_3L	27.20±0.11	35.83
CuH_2L	24.12±0.01	31.43
CuHL	19.46±0.02	23.71
CuL	11.90±0.03	15.86
$CuH_{-1}L$	3.44±0.03	7.41
$CuH_{-2}L$	-5.41±0.03	-2.58
$CuH_{-3}L$	-15.37±0.03	-13.65
$CuH_{-4}L$	-25.71±0.03	-
$\log\beta_{CuH4L} - \log\beta_{CuH3L}$	-	3.77
$\log\beta_{CuH3L} - \log\beta_{CuH2L}$	3.08	4.40
$\log\beta_{CuH2L} - \log\beta_{CuHL}$	4.66	7.72
$\log\beta_{CuHL} - \log\beta_{CuL}$	7.56	7.85
$\log\beta_{CuL} - \log\beta_{CuH-1L}$	8.46	8.45
$\log\beta_{CuH-1L} - \log\beta_{CuH-2L}$	8.85	9.99
$\log\beta_{CuH-2L} - \log\beta_{CuH-3L}$	9.96	11.07
$\log\beta_{CuH-3L} - \log\beta_{CuH-4L}$	10.34	-

Table S2. Spectroscopic data for Cu^{2+} complexes with [His^{1,6}]OXT and [His^{1,6}]AVP.

[His^{1,6}]OXT							[His^{1,6}]AVP						
	UV-VIS		CD		EPR			UV-VIS		CD		EPR	
	λ(nm)	ε ($M^{-1}cm^{-1}$)	λ(nm)	Δε ($M^{-1}cm^{-1}$)	A_{II}(G)	g_{II}		λ(nm)	ε($M^{-1}cm^{-1}$)	λ(nm)	Δε($M^{-1}cm^{-1}$)	A_{II} (G)	g_{II}
CuH_3L	-		-		-		CuH_4L	730	25	-		144	2.375
CuH_2L	671.5	53	303	-0.2317	162	2.281	CuH_3L	671.5	35	-		-	
			328.5	0.0620									
			340	-0.0620									
CuHL	643	71	277.5	-0.071	168	2.260	CuH_2L	632	92	242	-4.5389	190	2.242
			303.5	-0.4703						293.5	-0.3140		
			329	0.1891						466	-0.1420		
			341.5	-0.0684						673	0.1338		
			732	0.269						782	-0.1911		
CuL	627	95	295.5	-0.8389	179	2.250	CuHL	-		-		-	
			329	0.5022									
			489	-0.2828									
			643.5	0.4004									
$CuH_{-2}L$	509	173	292	-1.2717	-		$CuH_{-1}L$	508.5	174	280	-3.3819	211	2.173
			327	0.9202						325	0.5630		
			510	-0.5740						532	-0.8448		
			636.5	0.3066									
$CuH_{-3}L$	-		-		-		$CuH_{-2}L$	507	188	282	-3.3819	210	2.170
										324	0.1755		
										361	-0.1639		
										532	-0.8448		
$CuH_{-4}L$	508.5	196	289	-0.5854	203	2.176	$CuH_{-3}L$	507	189	288	-2.6732	208	2.170
			325.5	0.6487						361	-0.1639		
			516.5	-1.0197						530	-1.7596		
			636.5	0.0258									

Table S3. Proton paramagnetic relaxation contribution (R_{1p}), Cu(II)–proton distances (r) for 3.2 mM and 2.8 mM [$His^{1,6}$]OXT and [$His^{1,6}$]AVP in the presence of 0.02 Cu(II) equivalents, respectively. pH = 6.0, T = 298 K, H_2O/D_2O (9:1, v:v) for both samples.

	R_{1p} (s^{-1})	r (Å)		R_{1p} (s^{-1})	r (Å)
[$His^{1,6}$]OXT + 0.02 eq. Cu(II)			[$His^{1,6}$]AVP + 0.02 eq. Cu(II)		
His6 $H^{\varepsilon 1}$	15,48	3.1	His6 $H^{\varepsilon 1}$	59,20	3.1
His1 $H^{\varepsilon 1}$	broad	3.1	His1 $H^{\varepsilon 1}$	64,53	3.1
His6 $H^{\delta 2}$	5,62	5.1	His6 $H^{\delta 2}$	7,76	5.1
His1 $H^{\delta 2}$	5,64	5.1	His1 $H^{\delta 2}$	7,80	5.1
Ile3 H^{N}	1,75	6.5	Phe3 H^{N}	9,67	4.9
Gln4 H^{N}	1,00	7.2	Gln4 H^{N}	0,45	8.3
His6 H^{N}	2,90	5.9	Phe3 H^{ε}	4,57	5.6
Leu8 H^{N}	1,17	7.0	Phe3 H^{δ}	1,75	6.6
Gly9 H^{N}	1,51	6.7	Phe3 H^{ζ}	8,66	5.0
Gln4 $H^{\varepsilon 2}$	0,09	11.0	Tyr2 H^{ε}	1,24	7.0
Asn5 $H^{\delta 2}$	0,24	9.2	Gln4 $H^{\varepsilon 2}$	0,97	7.3
Tyr2 H^{δ}	9,28	4.4	Asn5 $H^{\delta 2}$	0,18	9.7
Tyr2 H^{ε}	9,86	4.3	Tyr2 H^{α}	2,30	6.3
His1 H^{α}	15,20	3.2	Phe3 H^{α}	0,76	7.6
Tyr2 H^{α}	1,36	6.8	Pro7 H^{α}	0,97	7.3
Ile3 H^{α}	0,38	8.5			
Asn5 H^{α}	1,17	7.0			
His6 H^{α}	5,62	5.1			
Pro7 H^{α}	0,79	7.5			
Leu8 H^{α}	0,54	8.0			
Pro7 H^{δ}	1,90	6.4			